DALTON
FULL PAPER

Structural and spectral diversities in copper(II) complexes of 2,6-bis(3,5-dimethylpyrazol-1-ylmethyl)pyridine ‡

Palanichamy Manikandan, K. R. Justin Thomas and Periakaruppan T. Manoharan *†

Department of Chemistry and Regional Sophisticated Instrumentation Center, Indian Institute of Technology, Madras, Chennai - 600 036, India. E-mail: ptm@magnet.iitm.ernet.in

Received 22nd March 2000, Accepted 21st June 2000
Published on the Web 28th July 2000

Copper(II) complexes of a tridentate nitrogen donor ligand, 2,6-bis(3,5-dimethylpyrazol-1-ylmethyl)pyridine (L), $CuLX_2$ (X = Cl, Br, NO_3, NCS or ClO_4) have been synthesized and characterized using UV-Vis and EPR spectra and electrochemistry. The EPR spectra reveal significant variations in a polycrystalline medium. Copper in all the compounds exhibits a stereochemistry close to a square based pyramid with trigonal bipyramidal distortion and the distortion is more pronounced in $CuL(NO_3)_2$. $CuLCl_2$ and $CuLBr_2$ crystallize in space group $C2/c$ and the molecules are arranged in the lattice such that they form columnar packing along the crystallographic a axis. $CuL(NO_3)_2$ crystallizes with space group $P2_1/c$ and forms discrete dimeric units through inter- and intra-molecular hydrogen bonding involving the nitro group and methyl and methylene groups. The polycrystalline EPR spectrum is characteristic of a triplet state. The electrochemical properties of these compounds are also discussed.

Introduction

Studies on copper compounds of chelating ligands incorporating pyridine, pyrazole, imidazole and benzimidazole have been of great interest in recent years.[1–13] This is mainly because of their relevance to the histidine co-ordinated copper proteins such as hemocyanin, tyrosinase, cytochrome c oxidase and laccase.[14–17] Very often better structural and functional models to metalloproteins have been prepared by altering the substituents of ligands in order to match with the required spectral properties of the metalloproteins.[1–7] In addition to easy handling, such manipulations are more feasible in pyridine and pyrazole co-ordinated ligands. Several pyridine based copper complexes reported by Karlin and co-workers and others have gained more importance in understanding of the electronic and co-ordination properties of copper proteins.[1–5] Kitajima *et al.* prepared pyrazole based copper complexes that proved to be better structural and functional models for hemocyanin and tyrosinase.[6,7] Sorrel and co-workers[11,18] have reported copper(I) complexes of pyrazole derived ligands to explain the non-reactivity of the CuB site of hemocyanin towards carbon monoxide. To give more insight into the co-ordination and electronic behaviours of pyridine and pyrazole based ligands with metal ions, we have embarked on a systematic study on copper complexes of a tridentate ligand, 2,6-bis(3,5-dimethylpyrazol-1-ylmethyl)pyridine (L), containing two pyrazoles and one pyridine donor.[19]

Studies of metal complexes of bis(pyrazolyl)pyridine ligands are of interest to us[19–22] and other groups.[23–26] Earlier we reported the synthesis and solution dynamics of the copper(I) compounds of L and L′ (2,6-bis(pyrazol-1-ylmethyl)-pyridine).[19,20] Herein, we report the synthesis and chelating properties of copper(II) compounds of the ligand L with different counter anions. In particular, our interest here is to uncover the electronic and steric effects of the two different heterocyclic moieties on the structural and spectroscopic properties of the copper(II) compounds. Crystal structures of three compounds $CuLCl_2$, $CuLBr_2$ and $CuL(NO_3)_2$ were determined and their geometrical parameters analysed critically.

† Honorary Professor, Jawaharlal Nehru Centre for Advanced Scientific Research, Bangalore, India.

‡ Electronic supplementary information (ESI) available: polyhedral angles, dihedral angles and calculated distortion parameters. See http://www.rsc.org/suppdata/dt/b0/b002289f/

Experimental

Physical measurements

X- and Q-band electron paramagnetic resonance (EPR) spectral measurements of these compounds were recorded on a Varian E-112 spectrometer, the g calibration being effected by diphenylpicrylhydrazyl (DPPH). Elemental analyses were done using a Heraeus CHN-O- rapid analyser. Electrochemical experiments were performed on a PAR 273 potentiostat/galvonostat interfaced with an IBM computer. A glassy carbon working electrode, a standard calomel electrode and a platinum plate auxiliary electrode constitute the conventional three-electrode cell assembly. Tetrabutylammonium perchlorate (0.1 mol dm^{-3}) was used as supporting electrolyte. The electrochemical behaviour of these compounds was examined by recording cyclic and differential pulse voltamograms in DMF solution.

Synthesis

CAUTION: although we have not had trouble with the perchlorate salts described, these compounds should be handled with appropriate precautions, as perchlorate salts are known for their potential hazards.

All solvents were obtained from commercial sources and dried and distilled prior to use by adopting standard procedures. 3,5-Dimethylpyrazole and pyridine-2,6-dimethanol were obtained from Aldrich Co. and used as received. 2,6-Bis(3,5-dimethylpyrazol-1-ylmethyl)pyridine (L) and $CuL(SCN)_2$ were prepared by adopting reported procedures.[19,22]

$CuLCl_2$ 1 and $CuLBr_2$ 2. To a solution of 0.295 g of L in 10 ml methanol was added an equivalent molar amount of $CuCl_2$ or $CuBr_2$ in 10 ml of methanol. The solution turned green immediately. After stirring for an hour, the solvent was allowed to evaporate slowly at room temperature (RT) to give green crystals. The yield was 90%. $C_{17}H_{21}Cl_2CuN_5$ requires C,

47.50; H, 4.92; N, 16.29%. Found: C, 47.64; H, 5.01; N, 15.98%. $C_{17}H_{21}Br_2CuN_5$ requires C, 39.36; H, 4.08; N, 13.5%. Found: C, 39.50; H, 3.98; N, 13.28%.

$CuL(NO_3)_2$ 3. To a solution of 0.188 g of $Cu(NO_3)_2{\cdot}6H_2O$ in 5 ml of methanol was added dropwise 0.295 g of L in 5 ml of methanol. The blue mixture was stirred for 30 minutes and then evaporated at room temperature to obtain 75% of product after recrystallization from methanol. $C_{17}H_{21}CuN_7O_6$ requires C, 42.28; H, 4.38; N, 20.30%. Found: C, 42.60; H, 4.30; N, 20.15%.

$CuL(NCS)_2$ 4.[22] To a solution of 0.576 g of compound **3** in methanol (20 ml) was added 0.076 g of NH_4NCS in 10 ml methanol with stirring. A green precipitate was formed. The mixture was allowed to stir for one hour to ensure complete conversion and filtered. The residue was washed with cold methanol–water (1 : 1) and recrystallized from acetonitrile. $C_{19}H_{21}CuN_7S_2$ requires C, 48.03; H, 4.46; N, 20.64%. Found: C, 47.75; H, 4.55; N, 20.50%.

$CuL(ClO_4)_2{\cdot}H_2O$ 5. To a solution of 0.295 g of L in 5 ml of methanol was added 0.37 g of $Cu(ClO_4)_2{\cdot}6H_2O$ dissolved in 5 ml of methanol with stirring. The reaction mixture immediately became dark blue. It was allowed to stir for an hour then the solvent was evaporated in vacuum. The resulting dark blue powder was recrystallized from methanol. Yield was 80%. $C_{17}H_{23}Cl_2CuN_5O_9$ requires C, 35.46; H, 4.03; N, 12.16%. Found: C, 36.01; H, 3.99; N, 12.23%.

Crystal structure determination of compounds 1, 2 and 3

Crystals of compounds **1**, **2** and **3** suitable for structure determination were mounted on a glass capillary using glue and transferred to an Enraf-Nonius CAD4 diffractometer. Unit cell dimensions were determined from 25 well centred reflections with $12 < \theta < 15°$. Data were collected using monochromatized Mo-Kα (0.71073 Å) radiation and corrected for Lorentz and polarization effects. An absorption correction was applied using ψ-scan data. Details of the X-ray data collection and refinement are given in Table 1. The structures were solved by direct methods and subsequent Fourier difference techniques (SHELXS 86[27]). Refinement on F^2 was carried out by full-matrix least-squares techniques (SHELXL 93[28]). Even though most of the hydrogen atoms were located from the Fourier difference maps they were included in the refinement at calculated positions (C–H 0.96 Å) riding on their respective parent atoms. All non-hydrogen atoms were refined with anisotropic thermal parameters while the hydrogen atoms were refined with overall isotropic thermal parameters. Atom scattering factors were taken from ref. 29. Definition of the bond angles (θ) in $CuLX_2$ complexes is illustrated in Fig. 1. Selected bond lengths and angles are listed in Table 2.

CCDC reference number 186/2049.

See http://www.rsc.org/suppdata/dt/b0/b002289f/ for crystallographic files in .cif format.

Results and discussion

Crystal structures

The chloro and bromo compounds **1** and **2** are isomorphous and isostructural. They crystallize in space group *C*2/*c*. The copper and pyridine nitrogen atoms lie on a crystallographic twofold axis of rotation symmetry. The molecular structure of **1** is displayed in Fig. 2 as representative. In these compounds copper is five-co-ordinated with three nitrogens from the capping tridentate ligand L and two halide ions, Cl in **1** and Br in **2** (Cu–Cl 2.3418(11) and Cu–Br 2.5139(5) Å).[30,31] The geometry around copper can be best described as square pyramidal where the basal plane is formed by two nitrogens of pyrazolyl groups and two halide atoms (Cl in **1** and Br in **2**).

Table 1 Crystal data and refinement details for the $CuLX_2$ compounds **1**, **2** and **3**

	$CuLCl_2$ **1**	$CuLBr_2$ **2**	$CuL(NO_3)_2$ **3**
Formula	$C_{17}H_{21}Cl_2CuN_5$	$C_{17}H_{21}Br_2CuN_5$	$C_{17}H_{21}CuN_7O_6$
Formula weight	429.84	518.74	482.95
Space group	*C*2/*c*	*C*2/*c*	$P2_1/c$
Crystal system	Monoclinic	Monoclinic	Monoclinic
T/K	298	298	298
Z	4	4	4
a/Å	7.911(3)	7.8585(11)	11.119(7)
b/Å	15.422(5)	15.843(8)	10.541(3)
c/Å	15.161(5)	15.4787(13)	17.650(4)
β/°	95.58(3)	97.401(9)	91.74(3)
V/Å^3	1840.8(11)	1911.1(10)	2067.7(14)
Total reflections	1744	1825	3814
Unique reflections	1620	1693	3615
No. of parameters	157	115	316
R_F [$I > 2\sigma(I)$]	0.0314	0.0304	0.0511
wR_F^2 [$I > 2\sigma(I)$]	0.0870	0.0768	0.1433

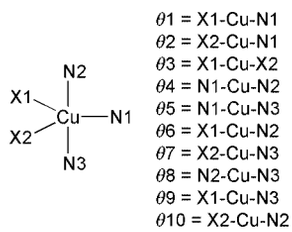

Fig. 1 Definition of the angles (θ) in $CuLX_2$ compounds.

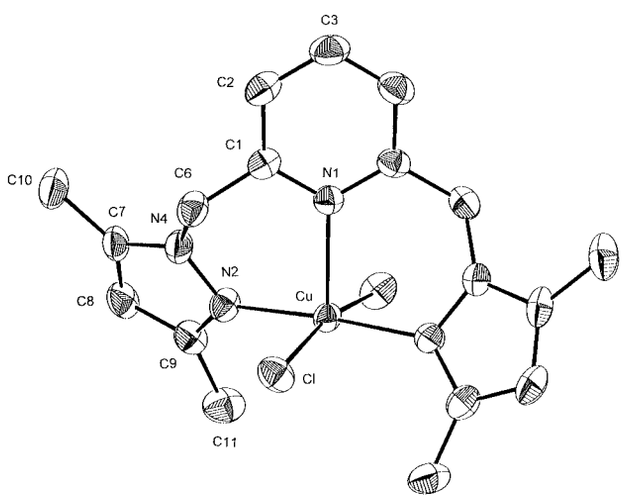

Fig. 2 Molecular structure and atom numbering scheme of $CuLCl_2$ **1**.

The pyridine nitrogen occupies the apical position in compound **1** at a rather long distance, 2.189(4) Å, and at 2.181(4) Å in **2**. The copper atoms are displaced from the basal plane in the direction of the Cu–$N_{pyridine}$ bond. The six-membered chelate ring N(1)C(1)C(6)N(4)N(2)Cu assumes a boat conformation. The interesting structural aspect of complexes **1** and **2** is their columnar packing leading to a quasi one dimensional chain. The rest of the arrays are dictated by crystal symmetry. The two neighbouring columns pack along the same direction but differ in the Cu–N_{py} orientation, being antiparallel to each other.

A perspective view of the compound $CuL(NO_3)_2$ **3** is shown in Fig. 3(a). The copper ion is five-co-ordinated with two pyrazolyl nitrogens, a pyridine nitrogen and one of the oxygens of the first nitrate group which constitute the basal plane, and the apical position is occupied by one of the oxygens of the second nitrate group. Thus the two nitrate groups function as monodentate ligands one with a short bond distance [Cu–O(1)

Table 2 Important bond distances (Å) and angles (°) for the $CuLX_2$ compounds

	$CuLCl_2$ **1**	$CuLBr_2$ **2**	$CuL(NO_3)_2$ **3**	$CuL(NCS)_2$ **4**[22]
Cu–X1	2.3418(11)	2.5139(5)	1.991(3)	1.997(4)
Cu–X2	2.3418(11)	2.5139(5)	2.294(4)	2.134(4)
Cu–N1	2.189(4)	2.181(4)	2.032(4)	2.070(3)
Cu–N2	1.985(3)	1.968(3)	2.019(4)	2.040(3)
Cu–N3	1.985(3)	1.968(3)	2.008(4)	2.039(3)
θ_1	97.01(3)	96.81(2)	168.5(2)	153.74(14)
θ_2	97.01(3)	96.81(2)	104.6(2)	106.40(13)
θ_3	165.99(5)	166.38(3)	86.84(14)	99.7(2)
θ_4	92.18(7)	92.76(9)	88.0(2)	86.54(11)
θ_5	92.18(7)	92.76(9)	90.0(2)	85.61(11)
θ_6	89.26(9)	89.21(9)	91.9(2)	87.51(14)
θ_7	89.26(9)	89.21(9)	92.7(2)	93.24(13)
θ_8	175.6(2)	174.5(2)	174.7(2)	169.10(12)
θ_9	90.21(9)	90.14(9)	89.0(2)	96.23(14)
θ_{10}	90.21(9)	90.14(9)	92.5(2)	96.22(13)
Δ	0.865	0.889	0.921	0.706
τ	0.161	0.135	0.103	0.256

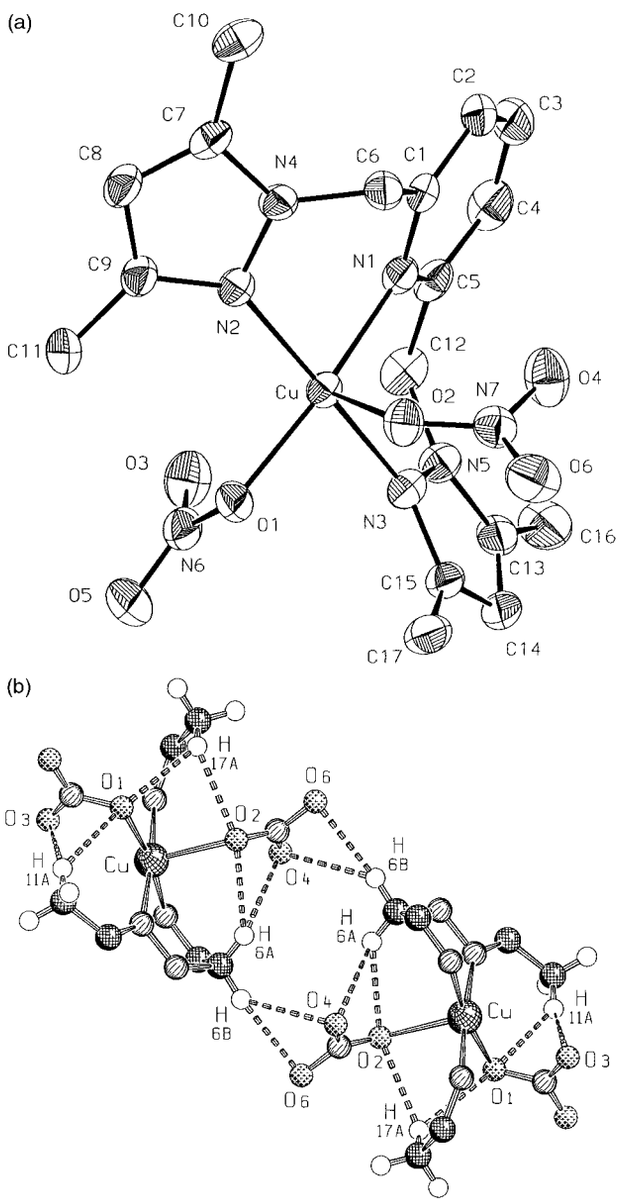

Fig. 3 (a) Molecular structure and atom numbering scheme of $CuL(NO_3)_2$ **3**. (b) Intra- and inter-molecular hydrogen bonding in **3**.

1.991(3) Å] and another with a significantly long bond distance [Cu–O(2) 2.294(4) Å]. The bond angle between the two co-ordinating oxygen atoms is 86.84(14)°. It is interesting that the basal plane consisting of N(1), N(2), N(3) and O(1) deviates significantly from planarity. The copper ion is raised 0.146 Å from the N(1)N(2)N(3)O(1) plane towards the apical nitrate oxygen. The dihedral angle between the basal plane and pyridine planes is 14.02(2)°. The six membered chelate rings adopt boat conformations. Analysis of the molecular packing of the complex indicates interesting C–H···O type intra- and inter-molecular hydrogen bonds between the oxygen atoms of the nitrato groups and the hydrogen atoms of the methyl and methylene groups. Oxygen atoms of the nitrato group at the equatorial position form intramolecular hydrogen bonding with the two proximal methyl groups. The oxygens of the nitrato group in apical position are involved in intramolecular hydrogen bonding with one of the proximal methyl and methylene groups and intermolecular hydrogen bonding with one of the methylene groups of the next monomer. In total, there exist three intramolecular bifurcated hydrogen bonds of the type C–H···O with bond distances and angles within the acceptable range (see Table 3 and Fig. 3b).[32] Thus the molecules aggregate as dimers in the crystal, formally linked by hydrogen bonds. The methylene hydrogen H6B is involved in bifurcated hydrogen bonding with the nitrato group of the adjacent molecule derived by the symmetry transformation $2 - x, -y, -z$. The copper–copper distance in this direction is 8.583 Å.

Comparison of compounds $CuLX_2$ (X = Cl, Br, NO_3 or SCN[22])

The most striking difference among the $CuLX_2$ compounds is the change in arrangement of the ligand around the metal centre that has occurred upon altering the exogenous monodentate ligands. In **1** and **2** the basal plane is constructed from two pyrazolyl donors of the ligand and two halide ions whereas in **3** and **4** this plane is composed of all the three N-donors of the ligand and one exogenous monodentate ligand. Even though the ligand in all the compounds co-ordinates in a *mer* conformation with two pyrazolyl groups in *trans* positions, the relative positions of the pyrazole and pyridine units with respect to the metal are also changed. In **1** and **2** pyridine occupies the apical position while in **3** and **4** it has moved to the equatorial position. These dissimilarities in spatial arrangements around copper arise as a result of the electronic and steric effects of the monodentate exogenous ligands. Apart from the different spatial configurations of the ligand donors

Table 3 Possible hydrogen-bonding interactions in compound $CuL(NO_3)_2$ **3** (distances in Å, angles in °)

Donor (D)	H	Acceptor (A)	D–H	H···A	D···A	D–H···A
C(6)	H(6A)	O(2)	0.9700	2.3887	3.1726	137.54
C(6)	H(6A)	O(4)	0.9700	2.5923	3.3418	134.21
C(6)	H(6B)	$O(4^{I})$	0.9700	2.5783	3.3340	134.85
C(6)	H(6B)	$O(6^{I})$	0.9700	2.4530	3.3847	160.95
C(11)	H(11A)	O(1)	0.9600	2.2764	3.0663	139.00
C(11)	H(11A)	O(3)	0.9600	2.4334	3.3093	151.58
C(12)	H(12A)	$O(5^{II})$	0.9700	2.5693	3.1356	117.34
C(17)	H(17A)	O(1)	0.9600	2.4856	3.1764	128.79
C(17)	H(17A)	O(2)	0.9600	2.4706	3.1836	130.97
C(17)	H(17C)	$O(4^{III})$	0.9601	2.5862	3.3186	133.26

Symmetry transformations: I $2-x, -y, -z$; II $1-x, -\frac{1}{2}+y, \frac{1}{2}-z$; III $2-x, \frac{1}{2}+y, \frac{1}{2}-z$.

and exogenous monodentate ligands around the copper atom, changes have also taken place in co-ordination distances as well. The copper to pyridine co-ordination bond distance (Cu–N(1)) is longer (2.189(4) Å and 2.181(4) Å) in **1** and **2** than in **3** (2.032(4) Å) and **4** (2.070(3) Å). Thus the four compounds can be divided into two categories. The two pyrazole to copper distances (Cu–N(2,3) increase on moving from **1** to **4** by approximately 0.06 Å whereas, the pyrazole–copper–pyrazole angle (θ_8) decreases by nearly 7.5°. As the copper to axial ligand distance increases (in the order **4** < **2** < **1** < **3**) the displacement of the copper from the mean basal plane decreases (in the order **3** < **2** < **1** < **4**).

We have calculated the dihedral angles between the polyhedral faces and the parameters Δ and τ by following the methods described by Meutterties and Guggenberger[33] and Addison *et al.*[34] The parameters Δ and τ describe the amount of deviation from trigonal bipyramidal geometry and trigonality respectively. For the regular square pyramidal structures the trigonality parameter τ will be zero, and it increases to 1.0 as the trigonal bipyramidal distortion increases. Similarly, Δ is zero for trigonal bipyramidal compounds and increases to 1.0 for square pyramidal (*SPY*) geometry. The calculated dihedral angles Δ and τ for the $CuLX_2$ compounds and related bis(pyrazole) ligand compounds are listed in Table 2. Among the four compounds considered in this study, **4** possesses a low Δ and high τ value. In the *SPY* extreme the nitrate derivative **3** possesses high Δ and low τ values. The variation of the Δ value for the compounds reported here is in the range 0.706–0.921 and τ is 0.103–0.256. The changes in Δ and τ values are 0.215 and 0.153. These observations suggest that all the compounds can be described as square pyramidal with varied degrees of trigonal bipyramidal distortion. The magnitude of Δ observed is in the order **3** > **2** > **1** > **4** and the reverse order is true for the variation in τ parameter. This indicates that compound **4** possesses more trigonal distortion in the series.

Spectroscopy

Infrared and UV-Vis. In the IR spectra the C–N stretching vibrations of the pyrazolyl and pyridine groups of the compounds show small shifts (≈5–10 cm^{-1}) from those of the "free" ligand due to their involvement in co-ordination. Compound **4** displays additional strong features at *ca.* 2060 cm^{-1} arising from the N-co-ordinated thiocyanate groups. Compound **5** shows broad absorption at 3500 cm^{-1} due to the presence of water. Bands due to the perchlorate ions are also noted in the spectra of **3**, however no information could be extracted from IR on their mode of attachment. For the co-ordinated NO_3^- group bands are seen at 1290, 1395 and 1471 cm^{-1}.

The optical spectra of the complexes are dominated by characteristic charge transfer bands in the near-UV region (Table 4). Besides the intense intraligand absorptions below 230 nm, associated with pyridine and pyrazole π–π* transitions, the spectra of the copper(II) compounds display two bands

Table 4 Electronic spectral data for the $CuLX_2$ compounds **1**–**5** in methanol (absorption coefficient in parentheses)

Compound	d–d band (cm^{-1})	LMCT (cm^{-1})
1 $CuLCl_2$	13,899(90)	29,851 (sh); 38,462 (6785)
2 $CuLBr_2$	13,699(115)	27,397 (sh); 38,462 (5990)
3 $CuL(NO_3)_2$	15,625(80)	30,769 (sh); 38,462 (6580)
4 $CuL(SCN)_2$	13,831(85)	24,570 (1103); 38,462 (sh)
5 $CuL(ClO_4)_2$	14,493(55)	29,412 (sh); 36,462 (6730)

near 38,462 and 29,412 cm^{-1} which can be attributed to π(pyrazole) ⟶ Cu^{II} and π(pyridine) ⟶ Cu^{II} LMCT transitions.[35] The thiocyanate compound (**4**) shows an additional intense band at 24,570 cm^{-1} arising from thiocyanate to copper charge transfer. All compounds exhibit a single unsymmetrical broad d–d band between 15,625 and 13,699 cm^{-1} indicating distorted square pyramidal structures.[35,36] For various anions the energy of the d–d transition increases in the order $Br^- < NCS^- \approx Cl^- < ClO_4^- < NO_3^-$. This suggests that the structure of the nitrate compound (**3**) is mainly square planar with weak axial interaction from oxygen of the other nitrate ion which is in line with the crystal structure determination (see below). Theories on the intensity of ligand field absorption bands predict that the intensity of the d–d transition increases as the symmetry of the ligand field decreases, since d–d transitions become allowed as electric dipole transitions.[37] A close inspection of Table 4 indicates that the intensities increase in the order **5** < **4** < **3** < **1** < **2** suggesting more trigonal distortion for the halide compounds (**1** and **2**) at least in solution. Hence, the ordering of the intensities and of the d–d energies is internally consistent. In addition, it is remarkable that the structural identity of the compound ion includes the anions even in solutions.

Electron paramagnetic resonance. *Polycrystalline spectra.* X-Band (≈9.4 GHz) EPR spectra of polycrystalline samples of compounds **1** and **2** at room temperature are orthorhombic in nature. The observed g values are $g_1 = 2.246$, $g_2 = 2.094$, $g_3 = 2.027$ and $g_1 = 2.222$, $g_2 = 2.114$, $g_3 = 2.039$ for $CuLCl_2$ and $CuLBr_2$ respectively. The large anisotropy in these values is indicative of a geometry distorted from the regular square pyramid for the CuN_3X_2 polyhedra in the solid state.[35,36] Similar observations have been made earlier for copper(II) compounds derived from the more rigid terpyridine ligand.[23,38] Substantial differences especially in the g values of compounds **1** and **2** arise from the enormously different 'spin–orbit coupling' constants of the halide ligands.[39] Variable temperature X-band EPR spectra were measured for these complexes in the temperature range 20–300 K on polycrystalline samples. They reveal, more or less, the same rhombicity throughout the temperature range with no change in the g values.

Table 5 Observed EPR parameters for the $CuLX_2$ compounds **1**–**5**

Compound	Medium	g_{av},g_{iso}	a_{iso}	g_1,$g_\perp$	g_2	g_3,$g_\parallel$	$A_\parallel^{Cu}$/ 10^{-4} cm^{-1}	$A_\perp^{N}$/ 10^{-4} cm^{-1}	G	$g_\parallel A_\parallel^{-1}$/ cm
$CuLCl_2$	Powder, RT	2.125	—	2.027	2.093	2.254	—	—	—	—
	Powder, LNT	2.124	—	2.027	2.092	2.252	—	—	—	—
	Methanol solution	2.140	60	2.060	—	2.299	170.6	14.42	4.98	134.8
$CuLBr_2$	Powder, RT	2.120	—	2.039	2.093	2.227	—	—	—	—
	Powder, LNT	2.127	—	2.041	2.105	2.236	—	—	—	—
	Acetonitrile solution	—	62	2.062	—	2.299	169.5	14.43	4.82	135.6
$CuL(NO_3)_2$	Powder, RT	—	—	2.072	—	[a]	—	—	—	—
	Powder, LNT	—	—	2.067	—	[a]	—	—	—	—
	Methanol solution	2.136	63	2.060	—	2.287	176.06	14.42	4.78	129.9
$CuL(NCS)_2$	Powder, RT	2.144	—	2.087	—	2.258	—	—	—	—
	Powder, LNT	2.143	—	2.085	—	2.258	—	—	—	—
	Methanol solution	—	—	2.097	—	[a]	[a]	14.05	—	—
$CuL(ClO_4)_2$	Powder, RT	2.117	—	2.056	—	2.239	—	—	—	—
	Powder, LNT	—	—	2.061	—	—	—	—	—	—
	Methanol solution	2.129	62	2.064	—	2.293	172.5	14.44	4.58	132.9

a_{iso} = Isotropic hyperfine coupling constant. [a] Precise value could not be obtained because of broadening.

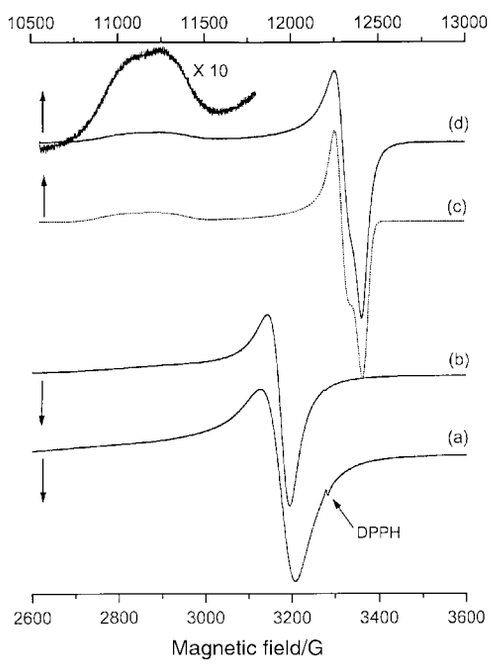

Fig. 4 X-Band polycrystalline EPR spectra of compound **3** at RT (a) and 77 K (b). The Q-band EPR at RT (d) with simulation (c) is also shown.

The dimeric nature of compound **3** is supported by EPR results. The X-band polycrystalline EPR spectrum exhibits axial symmetry with broad $g_\perp$ signal ($\Delta B_{pp} = 80$ G) and poorly resolved $g_\parallel$ component at RT (Fig. 4). When the sample is cooled to 77 K the pattern remains the same except that the $g_\perp$ signal is narrowed considerably ($\Delta B_{pp} = 63$ G) possibly due to exchange interaction. The exchange interaction, if any, should be between the copper centres of the hydrogen bonded dimeric unit. This is brought out by Q-band EPR studies. The Q-band spectrum of the above sample at RT not only clearly separates the signals of different g values but also shows a broad doublet on the $g_\parallel$ line and a distinct doublet in the $g_\perp$ region as shown in Fig. 4. These doublets are attributed to zero-field splitting arising out of a triplet state. This triplet state Q-band EPR spectrum was simulated using a program GNDIMER written by Smith and Pilbrow employing the Hamiltonian[40] (1). The zero-field splitting term (D) was calculated as the distance between the interacting centres. The dipolar component can be calculated using the formula[41] (2).

$$H = \beta H \cdot g \cdot S + D[S_z^2 - \tfrac{1}{3}S(S+1)] \quad (1)$$

$$D^{dipole} = 0.433\, g_z^2/r^3\ (\text{cm}^{-1}) \quad (2)$$

The spin-Hamiltonian parameters used for simulation were $g_\perp = 2.0558$, $g_\parallel = 2.2805$ and $r = 7.6$ Å ($D^{dipole} = 0.0051$ cm^{-1}). The crystal structure indicates the shortest Cu···Cu distance in this hydrogen bonded dimer is 8.583 Å. Further, the two adjacent molecules are linked by hydrogen bonds forming an exchange coupled dimer. Hence, the multiple hydrogen bond linkage between the two Cu^{II} of this complex in the solid state provides an efficient super exchange pathway as shown in Fig. 3(b) and as revealed by the triplet state EPR spectrum measured at Q-band frequency (Fig. 4). A detailed temperature dependent magnetic study of this interesting compound is in progress.

The X-band polycrystalline EPR spectra of compound **4** are essentially broad and asymmetric both at RT and LNT (liquid nitrogen temperature). The tailing in the low field region must be due to an unresolved $A_\parallel$ component that may be manifested clearly on dilution. The observed EPR parameters are given in Table 5. For all the complexes with nitrogen, oxygen or halogen co-ordination, the presence of the lowest 'g' value greater than 2.025 is consistent with a geometry closer to a square pyramid and the unpaired electron located essentially in $d_{x^2-y^2}$ based molecular orbitals.[36]

Liquid solution and frozen glass spectra. The X-band EPR spectra of all the complexes reveal perturbations in solutions although the variation is very significant in a polycrystalline medium. All complexes exhibit an isotropic signal with hyperfine splitting due to copper ion in free solution at RT and frozen solutions exhibit axial spectra (Fig. 5). All the complexes display superhyperfine splitting due to three co-ordinated nitrogens in the $g_\perp$ region though in the case of $CuL(NCS)_2$ and $CuL(ClO_4)_2 \cdot H_2O$ it is not manifested strongly. The frozen solution X-band EPR spectrum of complex **3** exhibits an axial character possessing $g_\parallel = 2.287$, $g_\perp = 2.060$ and $A_\parallel^{Cu} = 176.06 \times 10^{-4}$ cm^{-1} and $A_\perp^{N} = 14.42 \times 10^{-4}$ cm^{-1}. Hence, the complex behaves only as a monomer in solution, but as a dimer in the crystal exhibiting weak exchange coupling mediated by hydrogen bonds.

An increase in $A_\parallel$ value on going from the chloro to the nitrate complex further reinforces the idea of weak axial ligation of the nitrate group in **3**. As the signals are broad for **3** its precise $A_\parallel$ value could not be calculated. The G values[36] for the solution spectra are found to be greater than 4.0 which indicates that the complexes are ionic. Partial dissociation of the complexes in solution leading to the formation of

Table 6 Electrochemical data for the $CuLX_2$ compounds **1**–**5**

Compound	E_{pc} [a]/V	E_{pa} [a]/V	$E_{1/2} = \frac{1}{2}(E_{pa} + E_{pc})$ [a]/mV	$\Delta E_p = E_{pa} - E_{pc}$ [a]/V	E_p [b]/V
$CuLCl_2$	−0.118	[c]	[c]	[c]	−0.0637
$CuLBr_2$	−0.114	0.024	−0.045	138	−0.0282
$CuL(NO_3)_2$	−0.182	−0.082	−0.132	100	−0.1130
$CuL(SCN)_2$	−0.174	−0.072	−0.123	102	−0.1046
$CuL(ClO_4)_2$	−0.160	−0.056	−0.108	104	−0.0928

[a] Data from cyclic voltammetry, scan rate 50 mV s^{-1}, 10^{-3} M sample dissolved in DMF, 10^{-1} M NBu_4ClO_4 as electrolyte. [b] Data from differential pulse voltammetry. Pulse width 0.5 mV, scan range 1 mV s^{-1}. [c] Irreversible.

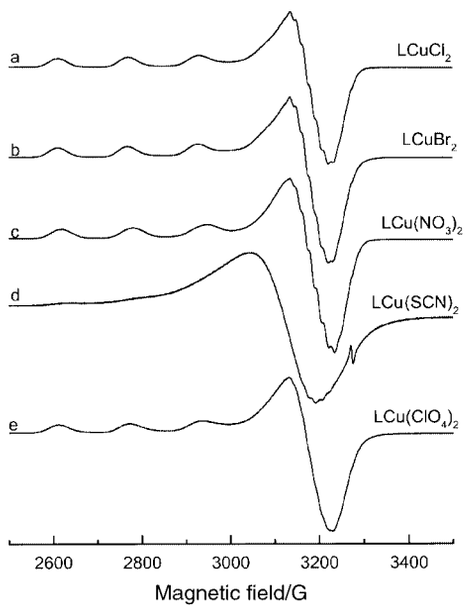

Fig. 5 X-Band EPR spectra (a)–(e) of compounds **1**–**5** respectively in methanol solution at 77 K.

solvated ionic complexes is also evident from the close resemblance of the spectra in solution. The quotient $g_{\|}/A_{\|}$ is proposed as a measure of tetrahedral distortion in tetragonal complexes.[42] For square planar structures the values occur in the range from 105 to 135 cm. This value increases significantly upon the introduction of a tetrahedral distortion in the co-ordination plane.

Electrochemistry

All the complexes undergo $Cu^{II} \longrightarrow Cu^{I}$ reduction in the potential range −0.114 to −0.182 V (Table 6). Interestingly, the chloro complex $CuLCl_2$ does not display a $Cu^{I} \longrightarrow Cu^{II}$ oxidation wave, suggesting that the copper(I) species generated is completely stable. The ΔE_p value of the bromo complex is much higher than that observed for other complexes. In general, the ΔE_p values of the complexes exceed the Nernstian value of 59 mV for a $n = 1$ process, indicating that their redox changes involve structural reorganization.[43]

The following important features emerge from the analysis of the Cu^{II}–Cu^{I} redox process: (i) the $E_{1/2}$ values of the complexes are in the order $CuLBr_2 > CuL(ClO_4)_2 \cdot H_2O > CuL(NCS)_2 > CuL(NO_3)_2$, which obviously reflect the Lewis basicity of the monodentate ligands, *i.e.* co-ordination of the more basic nitrate ligand reduces the acidity of the copper(II) complex and makes the reduction harder; and (ii) a constant value of i_{P_c}/i_{P_a} close to 1.0 was observed for all the complexes except the chloro derivative at 50 mV s^{-1} scan rate and remained almost unchanged on increasing the scan rate. Also the ΔE_p value increases progressively on increasing scan rate. These observations suggest that the Cu^{II}–Cu^{I} redox couple in the complexes is quasi-reversible. Greater irreversibility in complexes **1** and **2** indicates that the expulsion of exogenous ligands, *i.e.* Cl (**1**) and Br (**2**), occurs during the reduction process.[43]

Acknowledgements

P. M. thanks the Council of Scientific and Industrial Research (CSIR), New Delhi, India for a fellowship. This work was financially supported by a CSIR grant awarded to P. T. M. Partial support of K. R. J. T. was received from the Young Scientist Scheme (SR/SY/C-11) of the DST, New Delhi.

References

1 R. A. Ghiladi, T. D. Ju, R. M. Kretzer, P. Moenne-Loccoz, A. S. Woods, R. J. Cotter and K. D. Karlin, *J. Inorg. Biochem.*, 1999, **74**, 140.
2 R. T. Jonas and T. D. P. Stack, *Inorg. Chem.*, 1998, **37**, 6615.
3 N. Wei, N. N. Murthy, Q. Chen, J. Zubieta and K. D. Karlin, *Inorg. Chem.*, 1994, **33**, 1953.
4 K. D. Karlin, R. W. Cruse, Y. Gultneh, A. Farooq, J. C. Hayes and J. Zubieta, *J. Am. Chem. Soc.*, 1987, **109**, 2668.
5 K. D. Karlin, M. S. Haka, R. W. Cruse and Y. Gultneh, *J. Am. Chem. Soc.*, 1985, **107**, 5828.
6 N. Kitajima, T. Koda, S. Hashimoto, T. Kitagawa and Y. Moro-oka, *J. Am. Chem. Soc.*, 1991, **113**, 5664.
7 N. Kitajima, K. Fujisawa, C. Fujimoto, Y. Moro-oka, S. Hashimoto, T. Kitagawa, K. Toriumi, K. Tatsumi and A. Nakamura, *J. Am. Chem. Soc.*, 1992, **114**, 1277.
8 S. C. Sheu, M.-J. Tien, M.-C. Cheng, T.-L. Ho, S. M. Peng and Y.-C. Lin, *J. Chem. Soc., Dalton Trans.*, 1995, 3503.
9 C. F. Martens, A. P. H. J. Shenning, M. C. Feiters, H. W. Berens, J. G. M. Van der Linden, G. Admiraal, P. T. Beurskens, H. Kooijman, A. L. Spek and R. I. M. Nolte, *Inorg. Chem.*, 1995, **34**, 4735.
10 S. Chen, J. F. Richardson and R. M. Buchanan, *Inorg. Chem.*, 1994, **33**, 2376.
11 T. N. Sorrell and M. L. Garrity, *Inorg. Chem.*, 1991, **30**, 210.
12 L. Casella, O. Carugo, M. Gullotti, S. Doldi and M. Frassoni, *Inorg. Chem.*, 1996, **35**, 1101.
13 L. Casella, E. Monzani, M. Gullotti, F. Gliubich and L. De Gioia, *J. Chem. Soc., Dalton Trans.*, 1994, 3203.
14 A. Volbeda and W. G. L. Hol, *J. Mol. Biol.*, 1989, **209**, 249.
15 E. I. Solomon, M. J. Baldwin and M. D. Lowery, *Chem. Rev.*, 1992, **92**, 521.
16 G. M. Brudvig, T. H. Stevens and S. I. Chan, *Biochemistry*, 1980, **19**, 5275.
17 C. T. Martin, R. H. Morese, R. M. Kanne, H. B. Gray, B. G. Mamström and S. I. Chan, *Biochemistry*, 1981, **20**, 5147.
18 T. N. Sorrell, V. A. Vankai and M. L. Garrity, *Inorg. Chem.*, 1991, **30**, 207.
19 P. Manikandan, Ph.D. Thesis, submitted to Indian Institute of Technology Madras, 1997.
20 P. Manikandan, B. Varghese and P. T. Manoharan, *J. Chem. Soc., Dalton Trans.*, 1996, 371.
21 P. Manikandan, M. S. Moni, B. Varghese and P. T. Manoharan, *J. Chem. Soc., Dalton Trans.*, 1998, 3219.
22 P. Manikandan, K. R. Justin Thomas and P. T. Manoharan, *Acta Crystallogr., Sect. C*, 2000, **56**, 308.
23 A. A. Watson, D. A. House and P. L. Steel, *Inorg. Chim. Acta*, 1987, **130**, 167.
24 S. Mahapatra and R. Mukherjee, *J. Chem. Soc., Dalton Trans.*, 1992, 2337.
25 T. K. Lal, R. Gupta, S. Mahapatra and R. Mukherjee, *Polyhedron*, 1999, **18**, 1743.

26 K. G. Orrell, A. G. Osborne, M. W. daSilva, M. B. Hursthouse and S. J. Coles, *Polyhedron*, 1997, **16**, 3003.
27 G. M. Sheldrick, *Acta Crystallogr., Sect. A*, 1990, **46**, 467.
28 G. M. Sheldrick, SHELXL 93, Program for Crystal Structure Refinement, University of Göttingen, 1993.
29 *International Tables for X-Ray Crystallography*, Kynoch Press, Birmingham, 1974, vol. IV.
30 G. A. Nicholson, J. L. Petersen and B. J. McCormick, *Inorg. Chem.*, 1982, **21**, 3274.
31 W. L. Driessen, R. A. G. De Graaff, F. J. Parlerlief, J. Reedijk and R. M. De Vos, *Inorg. Chim. Acta*, 1994, **216**, 43.
32 J. B. J. Veldhuis, W. L. Driessen and J. Reedijk, *J. Chem. Soc.*, *Dalton Trans.*, 1986, 537.
33 E. I. Meutterties and L. J. Guggenberger, *J. Am. Chem. Soc.*, 1974, **96**, 1748.
34 A. W. Addison, T. N. Rao, J. Reedijk, J. van Rijn and G. C. Verschoor, *J. Chem. Soc.*, *Dalton Trans.*, 1984, 1349.
35 E. Bernarducci, W. F. Schwindiger, J. L. Hughey IV, J. Kroghjespersen and H. J. Schugar, *J. Am. Chem. Soc.*, 1981, **103**, 1686.
36 B. J. Hathaway, *Struct. Bonding* (*Berlin*), 1984, **57**, 55.
37 C. J. Ballhausen, *Introduction to Ligand Field Theory*, McGraw-Hill, New York, 1963, pp. 108–185.
38 W. Henke, S. Kremer and D. Reinen, *Inorg. Chem.*, 1983, **22**, 2858.
39 U. Sakaguchi and A. W. Addison, *J. Chem. Soc.*, *Dalton Trans.*, 1979, 600.
40 T. D. Smith and J. R. Pilbrow, *Coord. Chem. Rev.*, 1974, **14**, 173.
41 N. Sreehari and P. T. Manoharan, *Mol. Phys.*, 1988, **63**, 1077.
42 M. I. Arritortua, J. L. Mesa, T. Rojo, T. Dubaerdemacker, D. Beltran-Porter, H. Stratmeier and D. Reinen, *Inorg. Chem.*, 1988, **27**, 2976.
43 P. Zanello, in *Stereochemistry of Organometallic and Inorganic Compounds*, ed. I. Bernal, Elsevier, Amsterdam, 1990, vol. 4, pp. 181–281.